Bull Volcanol (2011) 73:55–72
DOI 10.1007/s00445-010-0403-6

RESEARCH ARTICLE

Spatio-temporal hazard estimation in the Auckland Volcanic Field, New Zealand, with a new event-order model

Mark S. Bebbington · Shane J. Cronin

Received: 17 December 2009 / Accepted: 23 August 2010 / Published online: 14 September 2010

Abstract The Auckland Volcanic Field (AVF) with 49 eruptive centres in the last c. 250 ka presents many challenges to our understanding of distributed volcanic field construction and evolution. We re-examine the age constraints within the AVF and perform a correlation exercise matching the well-dated record of tephras from cores distributed throughout the field to the most likely source volcanoes, using thickness and location information and a simple attenuation model. Combining this augmented age information with known stratigraphic constraints, we produce a new age-order algorithm for the field, with errors incorporated using a Monte Carlo procedure. Analysis of the new age model discounts earlier appreciations of spatio-temporal clustering in the AVF. Instead the spatial and temporal aspects appear independent; hence the location of the last eruption provides no information about the next location. The temporal hazard intensity in the field has been highly variable, with over 63% of its centres formed in a high-intensity period between 40 and 20 ka. Another, smaller, high-intensity period may have occurred at the field onset, while the latest event, at 504±5 years B.P., erupted 50% of the entire field's volume. This emphasises the lack of steady-state behaviour that characterises the AVF, which may also be the case in longer-lived fields with a lower dating resolution. Spatial hazard intensity in the AVF under the new age model shows a strong NE-SW structural control of volcanism that may reflect deep-seated crustal or subduction zone processes and matches the orientation of the Taupo Volcanic Zone to the south.

Keywords Monogenetic volcanism · Basaltic volcanic fields · Probabilistic hazard · Tephrostratigraphy

Editorial responsibility: J.D.L. White

M. S. Bebbington (✉) · S. J. Cronin
Volcanic Risk Solutions, Massey University,
Private Bag 11222,
Palmerston North 4442, New Zealand
e-mail: m.bebbington@massey.ac.nz

M. S. Bebbington
Institute of Fundamental Sciences—Statistics, Massey University,
Palmerston North, New Zealand

Introduction

The estimation of hazard in regions of distributed small-volume basaltic volcanism (monogenetic volcanic fields) is fraught with the challenges of understanding both the past frequency of eruption events and the order of events in relation to their spatial distribution (Connor and Hill 1995; Condit and Connor 1996; Conway et al. 1998). Such areas of volcanism are common to most parts of the Earth, and occur in a range of tectonic environments (Takada 1994; Valentine and Gregg 2008). Since the next eruption of a monogenetic field will most probably occur in a new location, any hazard forecast must consider not only the probability of when eruptive activity will resume, but also where. In urbanised volcanic fields, such as the 1.4 million population Auckland City, New Zealand, or locations with a high amenity/infrastructure value, such as the proposed Yucca Mountain Nuclear Waste Repository in Nevada, the question of where new eruptions may occur is especially critical for socio-economic risk assessment (Connor et al. 2000; Magill et al. 2005). These spatio-temporal relationships are also highly important to the understanding of the fundamental structure of volcanic fields and the processes behind distributed volcanism (Connor and Conway 2000).

Key hindrances to developing a hazard forecast for monogenetic field volcanism include establishing the ages

and frequency of past eruptions. This is especially true in Late Quaternary volcanic systems, such as the AVF, where a combination of young lavas with low-K composition (1.3–1.7% K_2O; Mochizuki et al. 2004) hinders application of Ar–Ar dating for the youngest eruptive products, and excess Ar in phenocrysts hampers conventional K–Ar dating (McDougall et al. 1969). Eruptions of field volcanoes are also often small, with very restricted deposits that frequently fail to overlap those of neighbouring centres. This reduces the chances of establishing a robust stratigraphic ordering. In addition, many volcanic fields, such as the AVF, display either little or conflicting evidence for structural control of vent locations (Spörli and Eastwood 1997; von Veh and Nemeth 2009), and a typical absence of obvious age:location trends. Because of these constraints the most common spatio-temporal hazard assessments for distributed volcanic systems rely on defining a vent clustering model (Magill et al. 2005), a structural/age model (Connor and Hill 1995; Cronin et al. 2001), or a geomorphology-based age model (Hasenaka and Carmichael 1985), or simply averaging the hazard over the field area.

In the Late Quaternary Auckland Volcanic Field (AVF; Fig. 1), 49 eruption centres occur over a 360 km^2 area, with well constrained location and volume information (Allen and Smith 1994). Age-dating in the field has, however, been extremely challenging, with one recent study (Lindsay and Leonard 2009) concluding that only nine of the eruptive centres can be dated with a high degree of reliability. Despite this fact, there is a large amount of other age-related information for the AVF that can be combined and used to build a robust age model and order events/locations. This includes dated tephras contained within sediment cores collected from a number of volcanic depressions in the region (e.g., Molloy et al. 2009). Geochemical correlation of these tephras to their source vents is made difficult by there being a low overall range of magma compositional variability in the field (Smith et al. 2009). In addition, individual eruptive centres/events may express a high degree of variability within the overall field range (cf. Smith et al. 2008) making unique correlations unlikely. A further limitation is the lack of available chemical datasets appropriate for correlation studies. The volcanic centres are represented dominantly by whole-rock analyses from lava flows or coherent bomb clasts (Smith et al. 2009), whereas the fine particle size in most tephra cores precludes representative whole-rock analysis and typically only glass chemistry is available (Molloy et al. 2009). Understanding these limitations, but using geochemistry as an aid where appropriate, we build a new age model for the AVF using a combination of (1) the known age constraints from the volcanic constructs from a range of sources; (2) all known physical stratigraphic relationships of volcanic products; and (3) a probabilistic correlation of dated tephra layers from sediment cores to their most likely volcanic source vents. This model shows major improvements in consistency over past attempts and, based on it, we present here a major re-evaluation of probabilistic hazard models for the field, along with new insights into its temporal and structural history.

Past dating of eruption centres in the AVF

Attempts at precisely dating AVF volcanoes began with the early application of ^{14}C methods (Fergusson and Rafter 1959) and have been carried out using a variety of radiometric techniques ever since, with varying degrees of success. Searle (1961) provided an early age-model, combining a few radiometric ages with stratigraphic and geomorphic constraints on some of the volcanoes. In the detailed mapping work of a number of workers, including Firth (1930), Searle (1959a, b, 1962, 1964, 1965) and later Kermode et al. (1992), field stratigraphic relationships are presented that assist in ordering the eruption events, even if not directly indicating their ages.

Allen and Smith (1994) summarized published and unpublished ages for the AVF in a comprehensive way, and this information has been recently updated by Lindsay and Leonard (2009). Both studies recognise the poor correlation between age estimates from different methods and conclude that few events are well constrained; the latter study classifying up to 35 eruption centres as without any form of reliable date. Part of the problem was recognised by McDougall et al. (1969) in that K–Ar ages from the field were considerably older than those provided by other means, due to excess Ar in the basaltic rocks. This was improved on by Mochizuki et al. (2004), and more recently still further with the application of incremental Ar–Ar dating (Cassata et al. 2008). Except for the most recently obtained of these ages, however, estimates vary greatly for the eruptions of single centres. The most consistent age determinations are from the ^{14}C method, especially where the organic material analysed was trapped (and charcoalised) beneath volcanic products. Notably, such ^{14}C ages are concordant with all of the newer Ar–Ar ages from the field.

In addition to dating studies, Rout et al. (1993) recognised that several of the volcanoes had products with similar magnetic field properties, implying coeval eruption. Cassidy (2006) went on to demonstrate that five eruptions (Crater Hill, Mt Richmond, Puketutu, Taylor Hill and Wiri Mountain) may have occurred during a period of no more than 100 years during the Mono Lake excursion (age ~29 ka). Cassata et al. (2008) also identified the Lashamp geomagnetic excursion and provided more precise ages for the eruptions during these two excursions. These ages appear to be consistent, within the error ranges, with the available ^{14}C ages.

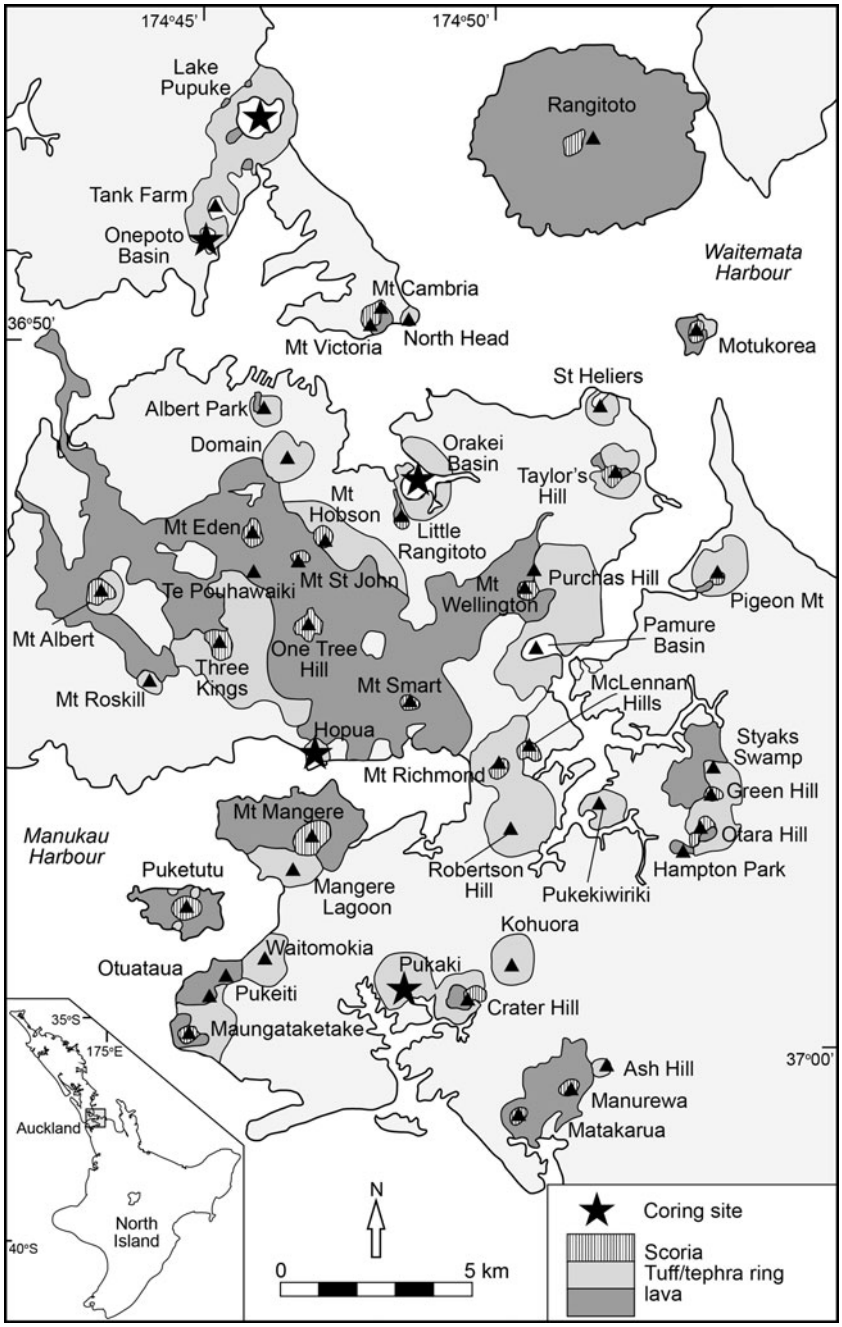

Fig. 1 Volcanic geological map of the Auckland Volcanic field, North Island, New Zealand, adapted from Kermode (1992), showing named volcanic centres and the major lithologies of eruptives. Coring sites for volcanic ash layers (Table 1) are located at: Lake Pupuke, Hopua, Orakei Basin, Onepoto Basin and Pukaki (indicated by *stars*)

Alongside the attempts to date individual eruption centres, an arguably even more reliable source of age information in the AVF has been derived from coring sediments within maar depressions throughout the field (Sandiford et al. 2001; Shane and Hoverd 2002; Molloy et al. 2009). There is, however, an absence of reliable geochemical information to link these determinations to particular eruptions. Hence, methods for combining core tephra dates (Turner et al. 2009) are not applicable. Shane and Hoverd (2002) combine a tephra record from Onepoto Basin with one from the Pukaki crater (Sandiford et al. 2001) to constrain the ages of 15 AVF events. Molloy et al. (2009) extended this to include records from Lake Pupuke, the Hopua Basin, and the Orakei Basin, detecting a total of 24 AVF events. Unfortunately, there is no evidence as to which volcano they correspond.

Constructing a new age model for the AVF

The cores collected in five locations (Fig. 1; Table 1) contain 24 tephras from the AVF (Molloy et al. 2009).

Table 1 Thickness and estimated age of AVF tephra in five cores, summarised from published data of Sandiford et al. (2001); Shane and Hoverd (2002); Molloy et al. (2009). Age errors are 1σ

ID	Thickness (mm)					Age (ka)				
	Pupuke	Onepoto	Orakei	Hopua	Pukaki	Pupuke	Onepoto	Orakei	Hopua	Pukaki
AV24	22					0.8±0.1				
AV23				3					10.0±0.7	
AV22					1					15.1±0.7
AV21				290	3				20.0±0.7	19.7±0.7
AV20				235	3				20.5±0.7	19.7±0.7
AV19					1					24.4±0.8
AV18			8	40	0.5			24.5±0.8	26.6±0.8	24.7±0.8
AV17			5					24.7±0.8		
AV16					50					25.5±0.8
AV15			12					26.7±0.9		
AV14			340					26.8±0.9		
AV13			740					26.9±0.9		
AV12	7	12	410	335	2	28.8±0.9	28.7±0.9	30.6±0.8	29.0±0.8	28.1±0.9
AV11					2					30.5±0.9
AV10	3					30.6±0.9				
AV9	6		400		850	30.8±0.9		31.5±0.8		
AV8	20	2	45		250	31.1±0.9	30.9±0.9	31.5±0.8		32.1±0.9
AV7	2	4	20		2	32.0±0.9	30.9±0.9	31.5±0.8		32.3±0.9
AV6		8			555		31.9±0.9			32.6±0.9
AV5			110					34.8±0.8		
AV4	15	12	35			34.4±0.9	35.0±0.9	35.4±0.8		
AV3			120					54.7±4.6		
AV2			510					68.3±6.4		
AV1		190	40				75.0±5.4	83.1±5.4		

These cores provide estimated dates that are constrained by deposition rates, ^{14}C determinations and tephrochronology of distal tephras from other North Island volcanoes. Geochemical correlation of the tephras to eruption centres has not been attempted because the inter-shard variation for the basaltic AVF tephras is high, precluding unique correlations to source cones (Shane and Hoverd 2002). Based on the unambiguous ages of the two most recent tephras, AV24 can be correlated to Rangitoto, and AV23 to Mt Wellington. To correlate the others to known sources we can make use of the known thickness, location, and stratigraphy, and in some cases the (^{14}C) age, which can be combined to assemble a coherent correlation model. Consider the relation

$$r = -1.85V^{1/3} + \exp[(8.67 + 1.13\log V - \log T)/2.38] \quad (1)$$

from Rhoades et al. (2002), where V is erupted volume of tephra (km^3), T is the deposited tephra thickness (cm), and r is the distance from the centre of deposit (km). We note that Eq. 1 is obtained by analysis of eruption volumes as small as 10^7 m^3, which is less than the average pyroclastic volume from events in the AVF. Although the model has corrections for wind effects, these are high-level winds, which are consistently from the West in New Zealand. However, dispersal from the 1–3 km altitude plumes assumed for the AVF is dominated by low-level winds which, judging by recent data (Reid 1980) exhibit none of the consistency of higher level winds. Although any given eruption will have occurred in a windfield, we have no information regarding the wind direction or strength, and so the least biased solution is to ignore wind correction terms, and assume the vents lie at the centres of deposits. We need simply to keep in mind that there will be wind errors, and that the derived correlations need to be tested further by geochemical or mineralogical methods when data become available.

In order to validate the relation (Eq. 1) for applicability to the AVF, including the insensitivity to wind effects, we will follow the approach of Magill et al. (2006), and examine the 1977 Ukinrek Maar eruptions, Alaska. These

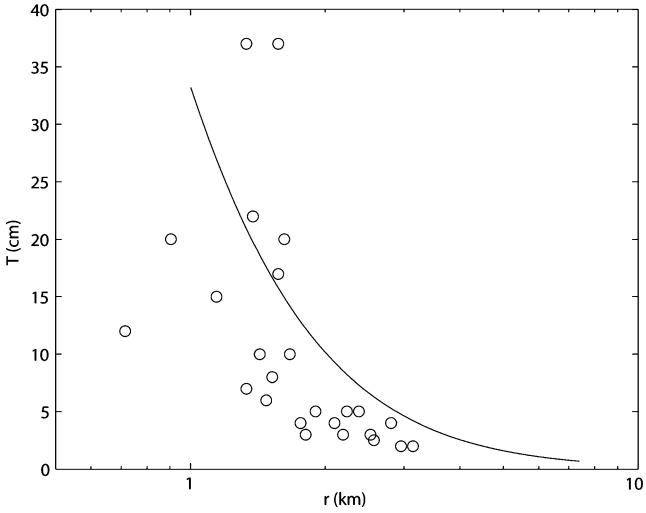

Fig. 2 Tephra thicknesses at distances from a point midway between the two vents of the 1977 Ukinrek Maars eruption, and the predicted relation (*solid line*) from Rhoades et al. (2002)

eruptions produced two maars with an estimated erupted volume of 0.026 km^3 (Kienle et al. 1980). Although the windfield (Fig. 4a of Self et al. 1980) exhibits a predominantly NNW and SE direction, the actual isopachs are almost circular (Fig. 1 of Self et al. 1980), indicating that at low levels, the wind correction may be neglected. Hence Fig. 2 shows the measured tephra thicknesses from Self et al. (1980), with radius distances measured from a point equidistant between the two vents, and the predicted thickness-distance relation from Eq. 1. This shows that the relation (Eq. 1) is reliable (cf. Magill et al. 2006), with possibly a tendency to under-estimate the distance for large volumes, and to over-estimate the distances for smaller volumes. However, the latter effect acts against the expected error due to omission of the wind correction, which we will bear in mind in our subsequent analysis.

Eruption volumes for each centre in the AVF were calculated by Allen and Smith (1994) using a number of methods:

1. If the area of the explosion crater was known, tuff volume was calculated as $(1/3)\pi r^2 h - \left(\pi r_c^2 h_t + (1/3)\pi r_c^2 (h - h_t)\right)$, where r is the radius of the tuff deposits plus the explosion crater, r_c the radius of the explosion crater, h the estimated (by extrapolation) height of deposits at the centre of the crater, and h_t is the height of the tuff ring.
2. Calculating the volume of country rock removed in the explosion crater from geophysical information, adding 30% for the magmatic content.
3. Using method 1 with the addition of a tuff base in cases where erosion eliminated distal tuff deposits.
4. Where limited data was available, using the formula $(1/3)\pi r^2 h$.

The resulting volume estimates range from ~10^{-4} km^3 (Pukeiti, Hampton Park and Purchas Hill) to 0.1014 km^3 (Three Kings), with a mean of 0.0137 km^3.

For each core listed in Table 1, and using the pyroclastic eruption volumes calculated by Allen and Smith (1994), the relationship (Eq. 1) can be used to construct graphs showing the thickness to be expected at each core site for each other eruptive centre in the field. An example for Pupuke is shown in Fig. 3. The multiple tephra thicknesses

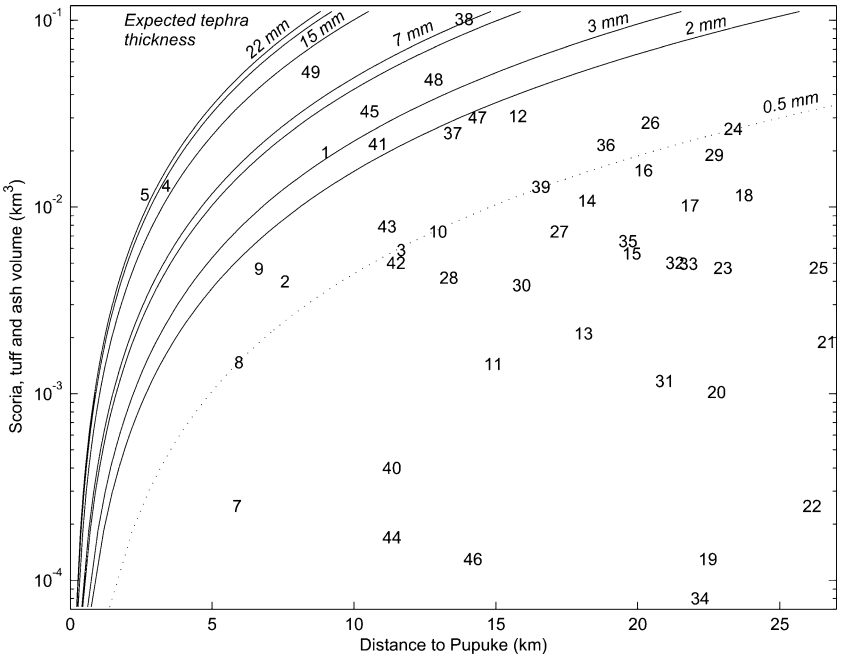

Fig. 3 Tephra attenuation curves for Pupuke core applying the relationship proposed by Rhoades et al. (2002). The numbers indicate the volume and distance of the vent, numbered according to the order in Allen and Smith (1994)—see Table 2. The curves show the combination of distance and volume expected to produce the observed tephra thickness at Pupuke. The *dotted curve* is for a thickness of 0.5 mm, which is considered the detection threshold, and *solid curves* proceed to the left, indicating thicknesses of 2, 3, 6, 7, 15, 20 and 22 mm

Table 2 New age model for the AVF, combining current known age constraints and geomorphology of the AVF volcanic structures and probabilistic correlation to tephra layers (as described in "Constructing a new age model for the AVF"), compared to the Allen and Smith (1994) assigned ordering of events. ^{14}C determinations are here considered to be the most reliable eruptive centre ages <30 ka B.P. and are deferred to if contrasting with results from other radiometric methods. Where multiple consistent ^{14}C ages are reported, the combined result and error is listed. Whole-rock K–Ar determinations are considered unreliable due to the presence of excess Ar in phenocryst phases (McDougall et al. 1969) and are hence excluded. Shaded units lack age constraints independent of tephra correlation

Order	Name	Age[a]	Error	Notes	Other Constraints	Tephra[v]
1	Domain	***68300***	***6400***	c	>60000	AV2
2	Albert Park				Heavily eroded[b]	
3	St Heliers				>>45000[d]	
4	Onepoto Basin	*248000*	*28000*	f	>42000[e]	
5	Tank Farm				>Onepoto?[b]	
6	Lake Pupuke	*200100*	*7400*	h	>45000[g], and >42000[e]	
7	Mt Cambria				=Mt Victoria?[b]	
8	Mt Victoria	***32200***	***1000***			AV10
9	North Head	***32700***	***1000***		>Mt Victoria?[b]	AV8[a,b]
10	Mt Albert	***34700***	***1400***	e	>Mt Roskill[b], Mt Eden[b], >30000	AV6[a]
11	Mt Roskill				>Three Kings	
12	Panmure Basin	32390	280	e,i		AV9
13	McLennan Hills	31690	180	i	*42600 ± 3800*[h]	
14	Mt Richmond	29910	600	j	= Crater Hill[h]	
15	Robertson Hill	***27200***	***1000***			AV17
16	Pukekiwiriki				>Styaks Swamp, >125000[b]	
17	Waitomokia	***27800***	***1000***		> Pukeiti[b]	AV16
18	Maungataketake	41390	430	e,i	>Otuataua, *38100 ± 1900*[k]	
19	Pukeiti				> Otuataua[b]	
20	Otuataua					
21	Matakarua	***15100***	***700***			AV22
22	Ash Hill	33800	160	l	>Wiri Mountain[b]	
23	Kohuora	*32000*	*2000*	m	>Crater Hill[b], >27000, c. 32000[m]	
24	Crater Hill	33970	280	b,e	*32100 ± 5400*[h]	AV6[c]
25	Wiri Mountain	30950	400	e,i	>Matakarua[b], = Crater Hill[h], *31000 ± 2700*[h]	AV11
26	Puketutu	*33600*	*3700*	h	= Crater Hill[h], *22800 ± 3300*[k]	AV8[c,d]
27	Pigeon Mt	***28200***	***1000***			AV15
28	Taylor's Hill				=Crater Hill[h]	
29	Pukaki	***83100***	***5400***	n	>65000	AV1[d]
30	Mt Smart	***21700***	***600***		>Mt Wellington	AV21
31	Styaks Swamp					
32	Green Hill	19827	8980	p	>Styaks Swamp[o]	
33	Otara Hill	***26700***	***1000***			AV19
34	Hampton Park	*26600*	*8000*	h	> Otara Hill[b]	
35	Mangere Lagoon	***27000***	***500***		>Mt Mangere[b]	AV18
36	Mt Mangere	21940	395	b,e	>Mt Smart[b], <27800 ± 1600[b], <30790 ± 290[d]	AV20
37	One Tree Hill	***37200***	***800***		>Three Kings, Hopua Basin, Mt Smart, Mt Eden, Mt Hobson[b], *17440 ± 1160*[q]	AV4
38	Three Kings	28590	381	r		AV12
39	Hopua Basin	***33700***	***1000***	d	>29000	AV7
40	Te Pouhawaiki				>Mt. Eden[b]	
41	Mt Eden	28390	345	s	>Mt Hobson, *15000 ± 1500*[q]	AV13
42	Mt St John	***54700***	***4600***	t	>Three Kings, Mt Eden[r], >23340± 450[d]	AV3
43	Mt Hobson	***28300***	***1000***			AV14
44	Little Rangitoto					
45	Orakei Basin			g	>Little Rangitoto[b], >83000	
46	Purchas Hill	10770	140	d	≥Mt Wellington fall[d]	
47	Mt Wellington fall	10520	80	b,e	>Mt Wellington Lava	AV23
47	Mt Wellington lava	10070	140	b,e		
48	Motukorea	***36600***	***1100***		>7000[b]	AV5
49	Rangitoto 1	552	g	d,u		AV24
49	Rangitoto 2	504	e	d,u		

[a] Reported in calibrated years B.P. for ^{14}C age determinations (CalPal Online; www.calpal.de) or tephrostratigraphic correlations based on radiocarbon chronology. Other types of age determinations are italicised. Bold italic indicates age determinations obtained from the tephra matching process

[b] Geomorphologically and stratigraphically based relative-age estimations are sourced from Firth (1930), Searle (1959a, b, 1961, 1962, 1964, 1965), Kermode et al. (1992), Allen and Smith (1994) and Affleck et al. (2001)

[c] Grenfell and Kenny (1995)

[d] Tephrostratigraphy, and some ^{14}C dates, Lindsay and Leonard (2009)

[e] Fergusson and Rafter (1959), Grant-Taylor and Rafter (1963, 1971)

[f] Shane and Sandiford (2003); whole lapilli Ar–Ar determination

[g] Molloy et al. (2009); tephrostratigraphy

[h] Cassata et al. (2008); Ar–Ar date no excess Ar reported

[i] Polach et al. (1969); McDougall et al. (1969)

[j] Sandiford et al. (2002)

[k] Wood (1991), thermoluminescence age on plagioclase crystals

[l] Hayward (2008)

[m] Newnham et al. (1999, 2007); tephrostratigraphy

[n] Shane (2005)

[o] Sibson (1968)

[p] Sameshima (1990)

[q] Combination of three TL ages from Adams (1986), Phillips (1989) and Wood (1991)

[r] Combination of six ^{14}C ages from Eade (2009)

[s] East and George (2003) radiocarbon age

[t] Horrocks et al. (2005b)

[u] Calibrated ages, combinations of several radiocarbon ages using OxCal 4.1 (c14.arch.ox.ac.uk; curve ShCal04), as reported in Lindsay and Leonard (2009)

[v] Tephra subscripts indicate the coring sites where they are described Onepoto (a), Pupuke (b), Pukaki (c), Orakei (d), and Hopua (e), see Table 1

of hundreds of mm mean that many of them must have been from sources within a few km, because there have been few events large enough to produce such thicknesses at distance, even allowing for the (unknowable) ambient winds and the tendency noted above for possible underestimation of distance in Eq. 1. Magill and Blong (2005) note that the median base surge area in the AVF is 2.63 km^2 and, at Ukinrek, thicknesses of 35–40 cm are found at distances of 1–2 km from the vents (Self et al. 1980). Another potential effect is possible over-thickening of some of the tephras within basins due to rainfall-induced remobilisation of tephra from the surrounding landscape. Secondly, events that appear to be recorded at Hopua and/or Pukaki in the south (Fig. 1), as well as Pupuke and/or Onepoto in the north, are likely to have been both large and central. Using these obvious starting points, we tested many various ways of assigning events to one of the 24 tephra layers. Dates directly from eruption centres (especially ^{14}C ages) that are considered reliable (Table 2) must of course match those tephra dates in Table 1 for any given assignment. In addition stratigraphic constraints (Table 2) must be respected. Further, all tephra layers have to be assigned. We also apply the assumption that an event cannot be identified with a tephra at a distal site, while being absent at a more proximal one on the same orientation. This effectively excludes the geological possibility of tephra erosion, but the depositional sites were lakes and most sequences show continuous sedimentation (e.g., Molloy et al. 2009). Hence, the chances of missing a proximal tephra in the record are very low. Combining these perspectives, the constraints on event identification become very tight, even allowing for a degree of subjectivity derived from the unknown wind effects.

The depositional ages of tephras in Table 1 were estimated (Molloy et al. 2009) by linear interpolation, and occasionally extrapolation, between marker tephras and ^{14}C dated horizons. As Molloy et al. (2009) provide no details of the precision of individual measurements within each core; this was estimated, for AV4-AV24, using a Monte Carlo procedure. In this procedure each control age was simulated from a normal distribution with standard deviation given by Lowe et al. (2008) or Molloy et al. (2009), and the interpolated ages recalculated. The estimated (1σ) error was then taken as the standard deviation from a sample of 1000 repetitions. However, there remains the error derived from the assumption of a constant sedimentation rate. We note that the estimated ages for those tephras considered by Molloy et al. (2009) as being present in at least three cores have standard deviations ranging from 0.5 ka to 1.2 ka. Hence we will use 0.7 ka, the mean of these, as a proxy for the error inherent in the linear approximation, which is combined with the precision error by adding the variances to obtain error estimates for each age. For AV1-AV3, the error was estimated as the sample standard deviations for the ages of the Eg10, Eg4 and Eg2 tephras (see Molloy et al. 2009) for AV3, AV2, and AV1 respectively. This last gives a somewhat larger estimated error than is claimed in Molloy et al. (2009), but as noted in the discussion in Molloy et al. (2009), these three ages are obtained by extrapolation rather than interpolation.

This does not, however, address the issue of systematic bias within a core, as exemplified by the differing age estimates in different cores for the same tephra. Hence, after a tephra has been correlated to a given eruption centre, that centre's (^{14}C) age is assigned to the tephra, and in a stepwise fashion used to 'calibrate' other ages estimated from the same core. Thus, and especially as we sometimes disagree with Molloy et al. (2009) about the common origin of different tephra deposits, we do not use the combined tephra ages across cores. Rather, we assume that each core has a systematic error, and estimate that via our correlation procedure. The assumed precision is then obtained by adding the variances in the assigned age and in the correlative age. In the case of multiple estimated ages from different cores, they are combined using the procedure of Ward and Wilson (1978). Turner et al. (2008b, 2009), proposed a different procedure for the tephra record at Mt Taranaki, using splines to estimate the sedimentation rate, and matching different cores via age distribution and principal component analysis of the tephra geochemistry.

Using the above methods and constraints, the AVF tephra correlation incorporates known age constraints, stratigraphic and geological criteria, with the final assignment of tephras to vents listed in Table 2. Note that some tephra layers correlated by Molloy et al. (2009) between sites in Table 1 were considered to be from different eruption centres, because of the wide separation in space or time, and conditional on previous assignments. The process of correlation proceeded as follows:

1. Exclude Onepoto (248 ka), Pupuke (200 ka), Orakei (>AV1), and Pukekiwiriki (> 125 ka) from consideration, because they are all older than the tephra sedimentary records.
2. Assign AV24 to Rangitoto, AV23 to Mt Wellington 1.
3. Assign AV12 to Three Kings, because it is present in all cores. Most likely this was sourced from a central location, and it was a large event. These criteria are most closely matched by Three Kings, which has also a well-fitting eruption centre age.
4. Assign AV13, 14 to Mt Eden and Mt Hobson, respectively. They are large tephras in Orakei, hence probably sourced from closely located vents, especially as they are not recorded elsewhere. Mt Eden and Mt Hobson have the desired stratigraphy, age, and location. Calibration of Orakei core ages by the Mt Eden ^{14}C date gives an age of 28.3±1.0 ka for Mt Hobson.
5. Assign AV4 to One Tree Hill, because it occurs in all northern cores and is the best combination of size, location and stratigraphy. This provides a calibrated age of 37.2±0.8 ka from the Hopua assigned age (see 14. below).
6. Assign AV11 to Wiri Mountain, since it is in only the Pukaki core and has the right age.
7. Assign AV9 to Panmure Basin, due to it being found in Pupuke, Orakei and Pukaki cores. Panmure Basin has the optimum location, size and eruptive style to have generated the observed tephra deposits, and is also approximately the right age.
8. Assign AV6 [in the Pukaki core] to the nearby Crater Hill, because it is a very large tephra with the right age. The 'Skip-over rule' means that AV6 [in the Onepoto core] must represent a different event.
9. Assign AV18, 20 and 21 to Mangere Lagoon, Mt Mangere and Mt Smart. This is the only feasible assignment that does not result in contradictions with later assignments; they are also consistent with locations and eruption volumes. Calibrated age for Mt Smart becomes 21.7±0.6 ka from the Mt Mangere ^{14}C age. The calibrated age for Mangere Lagoon becomes 27.0±0.5 ka from the Mt Eden and Mt Mangere ^{14}C ages.
10. Assign AV8 [in the Orakei and Pukaki cores] to Puketutu, due to it having the correct age, location and size. AV8 [in the Pupuke and Onepoto cores] appears to be a different event.
11. Assign AV16 to Waitomokia, because it is the only likely location remaining. The calibrated age estimate of this event is then 27.8±1.0 ka from the Mangere Lagoon assigned age.
12. Assign AV8 [in the Pupuke and Onepoto cores] to North Head, applying the skip-over rule. This provides a calibrated age of 32.7±1.0 ka from the Panmure Basin ^{14}C age.
13. Assign AV10 to Mt Victoria, applying the skip-over rule. This implies a calibrated age of 32.2±1.0 ka from the Panmure Basin ^{14}C age.
14. Assign AV7 to Hopua, due to its central location, size and minimum age. The calibrated age will hence be 33.7±1.0 ka from the Crater Hill ^{14}C age.
15. Assign AV2 to Domain, as the distance–thickness relationship at Orakei is consistent with the eruption from Domain, and the estimated tephra age exceeds the age constraint on Domain of >60 ka. Age is estimated at 68.3±6.4 ka.
16. Assign AV5 to Motokorea, because it is the only event with a thickness–distance relationship matching that of AV5 left unassigned, and Motokorea's low SiO_2 content matches the glass chemistry of AV5 rather than AV3 (Molloy et al. 2009, Fig. 7a). This results in a calibrated age of 36.6±1.1 ka from the One Tree Hill age assignment.
17. Assign AV3 to Mt St John, which is the best possibility remaining, resulting in an estimated age of 54.7±4.6 ka.

18. Assign AV1 [in the Orakei core] to Pukaki, with an estimated age of 83.1±5.4 ka.
19. Assign AV6 [in the Onepoto core] to Mt Albert (the only other possibility is Albert Park, where the high degree of erosion and weathering is inconsistent with the ~34 ka age estimated for AV6). This results in a calibrated age of 34.7±1.4 ka from the Hopua assigned age.
20. Assign AV15 and 17 to Pigeon Mountain and Robertson Hill, respectively. Any alternative remaining candidate source vents are either too old or located too far south. This results in a calibrated age of 28.2±1.0 ka for Pigeon Mountain from the Mt Eden ^{14}C age and 27.2±1.0 ka for Robertson Hill from the Mangere Lagoon assigned age.
21. Assign AV22 to Matakarua, resulting in an estimated age of 15.1±0.7 ka.
22. Assign AV19 to Otara Hill, giving a calibrated age of 26.7±1.0 ka from the Mangere Lagoon age assignment.
23. The only remaining source compatible with AV1 [in the Onepoto core] (190 mm) is Tank Farm. As the stratigraphy here is uncertain (Ian Smith, pers. comm.), we will accept this, with an assigned age of 75.0±5.4 ka. The only other possibility is a conjectured second phase of Pupuke (Ian Smith, pers. comm.).

The augmented age information from the assignment routine is shown in Table 2.

From this process we now have assigned ages for 39 out of 51 events (49 vents, with multiple eruptions at Mt Wellington and Rangitoto). Of the remaining 12 events, Taylor's Hill is considered equivalent in age to the Crater Hill group, based on paleomagnetism (Cassata et al. 2008) and Mt Cambria may be of very similar age to its partly coalesced neighbour Mt Victoria. Stratigraphic relationships can be used to bound the ages of five further centres (Mt Roskill, Pukeiti, Otuataua, Styaks Swamp and Little Rangitoto), assuming that the only centre younger than Mt Wellington is Rangitoto. Stratigraphic relationships provide lower bounding ages for another four centres (St Heliers, Pukekiwiriki, Te Pouhawaiki and Orakei Basin). Albert Park has no useable stratigraphic correlations and is only assumed to be one of the earliest eruptions in the field, based on its degree of weathering and subdued geomorphology (Searle 1962).

Description of AVF temporal behaviour

The result of "Constructing a new age model for the AVF" is an age or event-order determination with quantifiable unknowns for the AVF. Based on this we can examine the behaviour of the field by repeated Monte Carlo simulation of the ages, analysis of the simulated ages, and calculation of the mean and variance of the results. Ages were assigned via the following simulation algorithm:

1. The 39 events with estimated ages and errors were assigned an age from a normal distribution with the given mean and error.
2. Mt Cambria is sampled from the same distribution as Mt Victoria, and Taylor's Hill from a normal distribution with average and error given by the sampled ages of Mt Richmond, Wiri Mountain, Puketutu and Crater Hill.
3. If the sampled ages violate the stratigraphy, new random values are drawn for all the affected events. Note that the tephra assignments generate additional implied stratigraphy within each core.
4. The remaining 11 events are finally assigned an age that is uniformly distributed between any upper and lower stratigraphic bounds, with an assumed upper bound of 270 ka or the age of Onepoto Basin, whichever is greater. The age of St Heliers is assumed to be at least 90 ka, and Albert Park is assumed to be older than St Heliers (although this cannot currently be verified with certainty).

The results of 1000 Monte Carlo simulations are shown in Table 3, ordered by mean age. Notable features are the decomposition into six 'early' events (Onepoto Basin, Albert Park, Lake Pupuke, Pukekiwiriki, St Heliers and Orakei Basin), followed by (in order) the 'intermediate' events of Pukaki, Tank Farm, Domain and Mt St John. Following there is a period, from around 40 ka to 20 ka, probably beginning with the Maungataketake eruption, containing 31 or more events. A period from 20 ka to 10 ka with a few poorly-defined events is followed by the eruptions of Purchas Hill, Mt Wellington and Rangitoto as the most recent events. Unfortunately, the Little Rangitoto event remains almost completely unconstrained, and Te Pouhawaiki is little better.

Hazard models for the AVF

The usual object of stochastic modelling in monogenetic fields is a spatio-temporal estimate of the likely timing and location of the next event (Connor and Hill 1995; Conway et al. 1998; Cronin et al. 2001; Martin et al. 2004). Eruptive volume is not generally considered, except when the spatial dimension is heavily discretized (Bebbington 2008). The hazard model we attempt to construct here is a probabilistic model with point process intensity $\lambda(x,t)$ such that the probability of an event in the time interval $(t, t+\Delta t)$ in an area of size ΔA (which includes x) is approximately $\lambda(x,t) \times \Delta A \times \Delta t$ for small ΔA, Δt.

The first problem is how to treat multiple phases of the same eruptive centre. While we have data on the two most recent examples (Mt Wellington and Rangitoto), geological studies of Searle and others (see Table 2 references)

Table 3 Monte Carlo ages and ordering from 1000 simulations of the new AVF age-order model with constraints described in "Description of AVF temporal behaviour". Order(AS94) indicates the order within Allen and Smith (1994)

Name	Mean age (ka)	Age error (ka)	Order (AS94)	Min order	Max order
Onepoto Basin	246.8	28.8	4	1	8
Albert Park	227.6	41.2	2	1	7
Lake Pupuke	200.2	7.3	6	1	8
Pukekiwiriki	195.1	44.2	16	1	8
St Heliers	182.3	53.0	3	2	8
Orakei Basin	178.5	55.8	45	1	7
Te Pouhawaiki	152.0	70.0	40	1	33
Little Rangitoto	92.3	57.7	44	2	46
Pukaki	83.4	5.5	29	7	11
Tank Farm	75.2	5.5	5	6	12
Domain	69.3	5.3	1	7	12
Mt St John	54.7	4.5	42	9	14
Maungataketake	41.4	0.4	18	11	15
One Tree Hill	37.4	0.7	37	12	17
Motukorea	36.1	0.9	48	13	20
Mt Albert	35.2	0.9	10	14	21
Kohuora	35.1	1.0	23	13	21
Crater Hill	34.1	0.3	24	15	22
Hopua Basin	33.6	0.4	39	18	23
Puketutu	33.0	0.5	26	19	25
North Head	32.9	0.4	9	19	26
Hampton Park	32.4	4.8	34	12	41
Panmure Basin	32.3	0.3	12	21	27
Taylors Hill	32.0	1.9	28	13	39
Mt Roskill	32.0	1.9	11	16	34
Ash Hill	31.8	0.2	22	21	30
McLennan Hills	31.7	0.2	13	22	30
Mt Victoria	31.5	0.6	8	22	33
Mt Cambria	31.4	1.2	7	16	38
Wiri Mountain	30.9	0.4	25	24	32
Mt Richmond	29.9	0.6	14	25	35
Three Kings	28.8	0.3	38	29	35
Mt Eden	28.4	0.3	41	31	36
Waitomokia	28.1	0.8	17	27	39
Mt Hobson	28.1	0.3	43	32	37
Pigeon Mt	27.7	0.4	27	33	39
Robertson Hill	27.2	0.4	15	34	40
Mangere Lagoon	26.7	0.4	35	36	41
Otara Hill	25.9	0.7	33	38	42
Pukeiti	22.3	4.2	19	30	46
Mt Mangere	22.1	0.4	36	39	44
Green Hill	21.9	7.1	32	12	46
Mt Smart	21.4	0.5	30	40	45
Otuataua	16.4	4.3	20	36	47
Styaks Swamp	15.9	5.1	31	14	47
Matakarua	15.1	0.7	21	42	46
Purchas Hill	10.8	0.1	46	45	47
Mt Wellington	10.5	0.1	47	48	48
Mt Wellington 2	10.1	0.1	50	49	49
Rangitoto	0.6	0.0	49	50	50
Rangitoto 2	0.5	0.0	51	51	51

indicate that there were probably multiple phases at several of the other centres, particularly Pupuke, Three Kings, and Mt Eden, for which we have no specific age information. Thus, including the second-events from only two sites (Mt Wellington 2 and Rangitoto 2) in the hazard estimation will bias both the temporal and spatial aspects. The best solution for these incomplete data is, hence, to model only the hazard of a new centre, and consider the 're-activation' of a previous centre separately, assuming that sufficient data can be assembled. Effectively, we suppose that from a geologic perspective, multiple phases from the same eruptive vent constitute the same hazard as a continuous eruption from the vent. Such multiple phase behaviour has been observed for historical eruptions, such as Cerro Negro, over periods of decades, or even longer (Hill et al. 1998).

Magill et al. (2005) model

Previous age models for the AVF were considered unreliable, which motivated Magill et al. (2005) to construct a spatial mixture renewal model, attempting to forecast only the location of the next eruption. This was based on the apparent tendency of eruptions in the AVF to cluster at distances <4,600 m. This approach reduced the reliance on age determination, although the order of the eruptions was all-important. Using the eruption order from Allen and Smith (1994), Magill et al. (2005) showed that the distance between consecutive vents was significantly smaller than that between all pairs of vents, concluding that eruptions do not occur randomly, but rather preferentially closer to the previous eruption. The distance of 4,600 m was then used to define clusters, with an eruption being assigned to the same cluster as the previous event if the distance between the two eruption centres was less than 4,600 m. This collapsed the 49 eruptions into 18 clusters.

In the above construction, the vent locations were justifiably considered known. Hence the regularity distance is unaffected by any errors in dating. Given that the cluster construction process used only the order of the eruptions (and not the ages) from Allen and Smith (1994), they supported a high degree of clustering. However, there appears to have been a tendency in the Allen and Smith (1994) age model to assign vents with undetermined age to a place in the order consistent with their close spatial neighbours (Ian Smith, pers. comm.), and thus there was an unintended circular dependence between clustering and ordering.

With the new age-order model, and applying the dating algorithm above for 1000 Monte-Carlo runs, considerable differences in eruption order emerge in comparison to the Allen and Smith (1994) model. First, if we consider the order given by the simulated mean age in Table 3, we see that the clusters identified by Magill et al. (2005) are no longer as evident (Fig. 4). Further, using the 1000 Monte Carlo run data (not the results in Table 3), the distribution

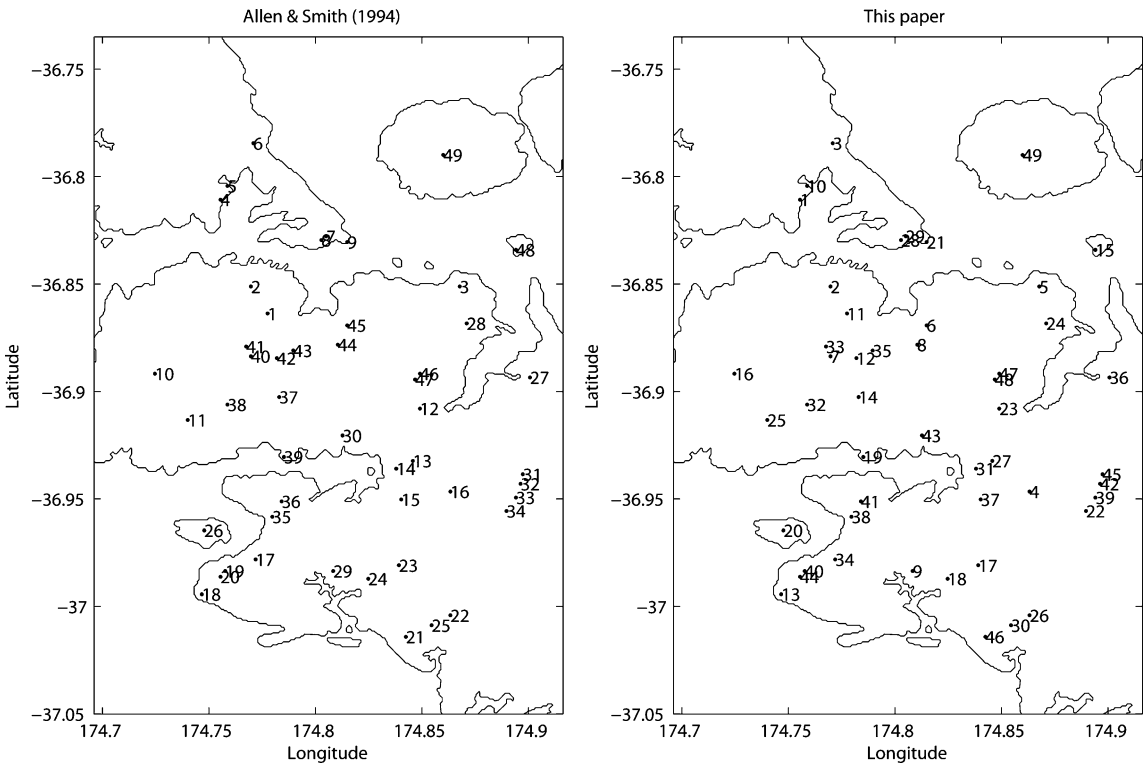

Fig. 4 Comparison of Allen and Smith (1994) and new eruption order for the AVF

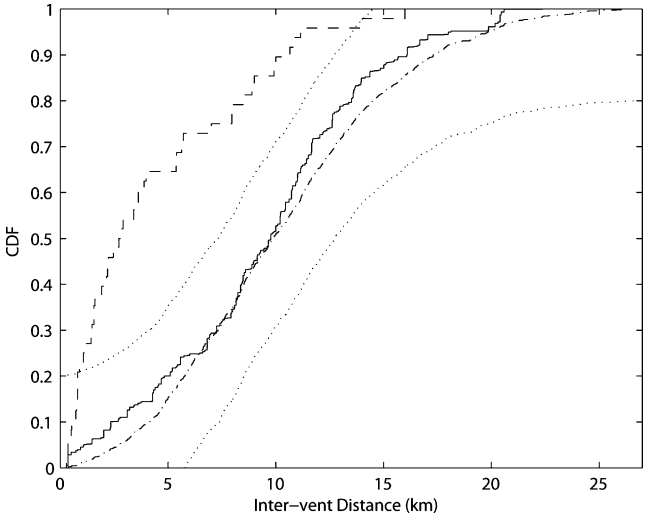

Fig. 5 Distances between successive eruption centres in the AVF. *Dashed line* is Allen and Smith (1994) order of events, the *solid line* represents 1000 Monte Carlo repetitions of the new age-order, the *dot-dashed line* is the result from all possible pairs, and the *dotted line* is a 95% confidence band based on the latter

function for the inter-vent distance between successive eruptions for the new age model is no longer significantly different to that between all pairs of centres (Fig. 5).

Spatio-temporal properties

As the assumptions behind the Magill et al. (2005) model no longer appear valid, a new estimate of the hazard is needed. This requires examination of the spatial and temporal structure of the data, including the distances and azimuths between successive events (Fig. 6). While the distance between all pairs of centres appears to be Weibull distributed (cf. Magill et al. 2005), there seems to be some evidence of more structure in the new Monte Carlo results, though this is influenced by certain order-pairs, such as Purchas Hill—Mt Wellington—Rangitoto, being present in most or all of the simulations. The all-pairs azimuth distribution, including its two preferred directions, appears to be reproduced in the new Monte Carlo simulated order, implying that there is little information about the direction of the next event that can be extracted from the location of the previous event.

The second order properties, i.e., the relationship of distances and azimuths between successive pairs of events, are shown in Fig. 7. The main pattern is a tendency to avoid the same azimuth between two successive pairs of events, and that the previous inter-centre distance provides no information about the next inter-centre distance. Overall, it appears that the location of the previous centre has no effect on the next centre, beyond those effects from the overall spatial structure of the field. Further, Fig. 8 shows that the temporal and spatial distances between successive events appear to be unrelated. This means that a spatio-temporal model with independent temporal and spatial terms is justified. Thus, we can decompose the point process intensity as $\lambda(x,t) = \lambda(t)f(x)$, and estimate the terms separately.

Temporal component of hazard

Figure 9 shows the temporal structure for the AVF, both between successive events and over the life of the field. The distribution of the inter-event times is not memoryless (i.e., a Poisson process), instead exhibiting a tendency to cluster at short time intervals. This obviously corresponds to the peak(s) in the kernel estimate of the eruption rate at about

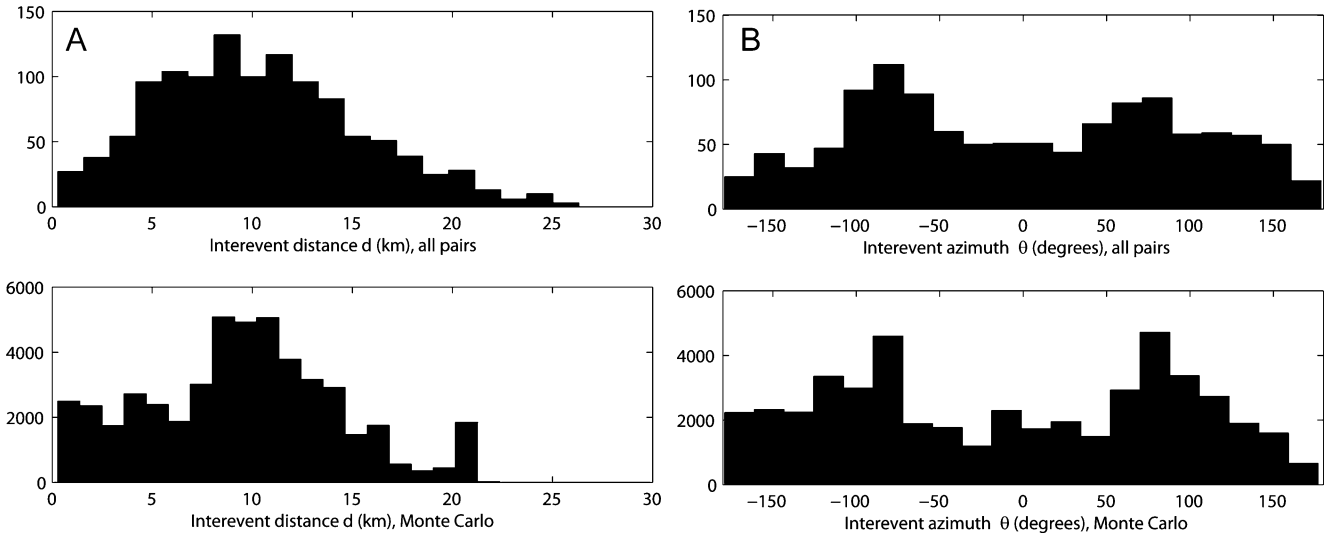

Fig. 6 Distances (**a**, km) and azimuths (**b**, degrees clockwise from East) between successive eruptions. Top plots show the result from all pairs of centres, whereas the bottom graphs are the result from 1000 Monte Carlo repetitions of the new dating algorithm

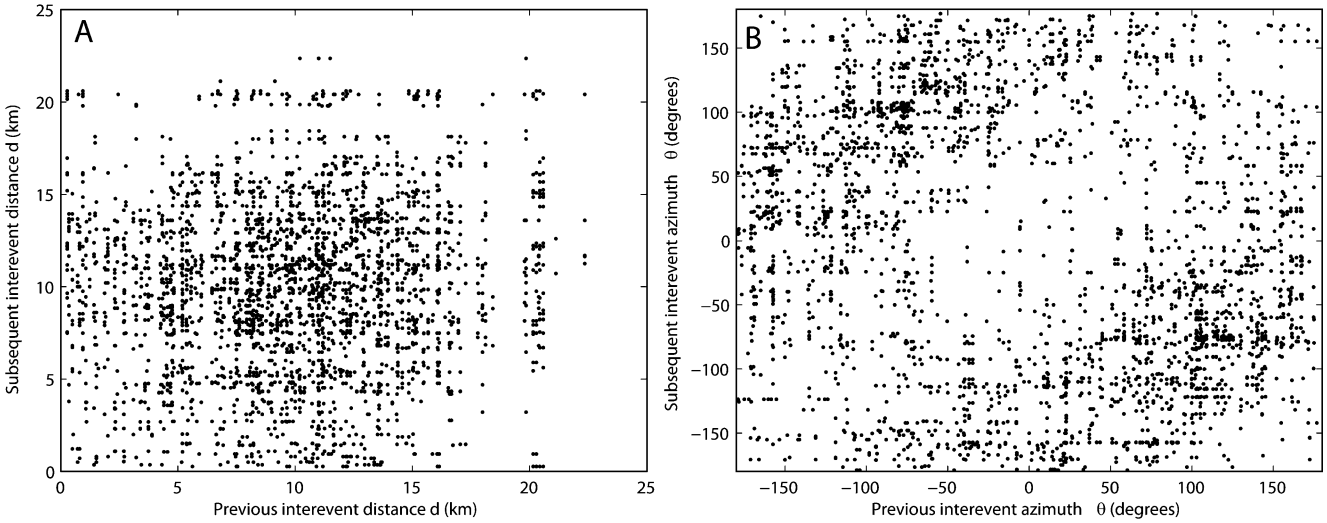

Fig. 7 Distances (**a**, km) and azimuths (**b**, degrees clockwise from East) between pairs of successive eruptions, 1000 Monte Carlo repetitions of the new dating algorithm

30 ka. The deviation from Poisson behaviour at longer intervals is a function of the sparse and imprecisely dated early record. The same effect is noticeable on a second order plot of successive inter-event times.

In defining the form of the temporal model component it must first be recognised that the process is clearly not stationary, and thus not a renewal model (Bebbington and Lai 1996). Also, the volume anomaly of Rangitoto (comprising up to 50% of the field volume in one centre; Kermode, 1992) makes a volume-dependent model (Bebbington 2008) infeasible. In addition, because there appears to be less than a full cycle in the intensity, a trend renewal model (Bebbington 2010), or a hidden Markov model approach (Bebbington 2007) is not feasible. However, the clustering at short intervals indicates that a triggering model might be appropriate.

Let us denote the event times as occurring at $t_1<t_2<\cdots<t_N$, where the observation period is $t \in (T_1, T_2)$, say, and assume that new eruptions occur at random in a

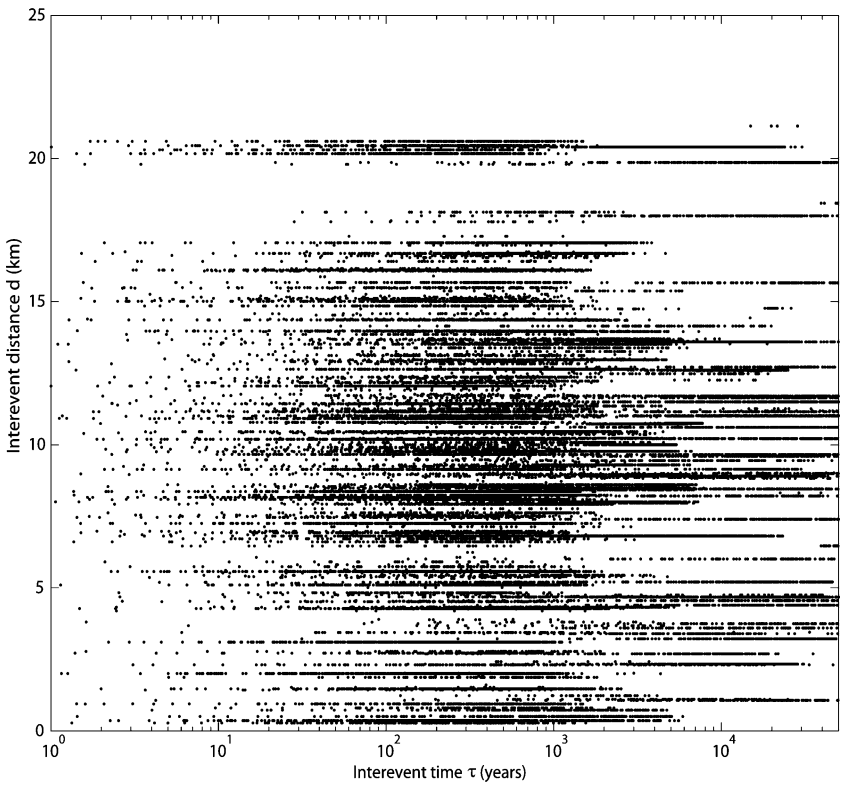

Fig. 8 Time versus distance between successive events (based on 1000 Monte Carlo simulations of the new age-order model)

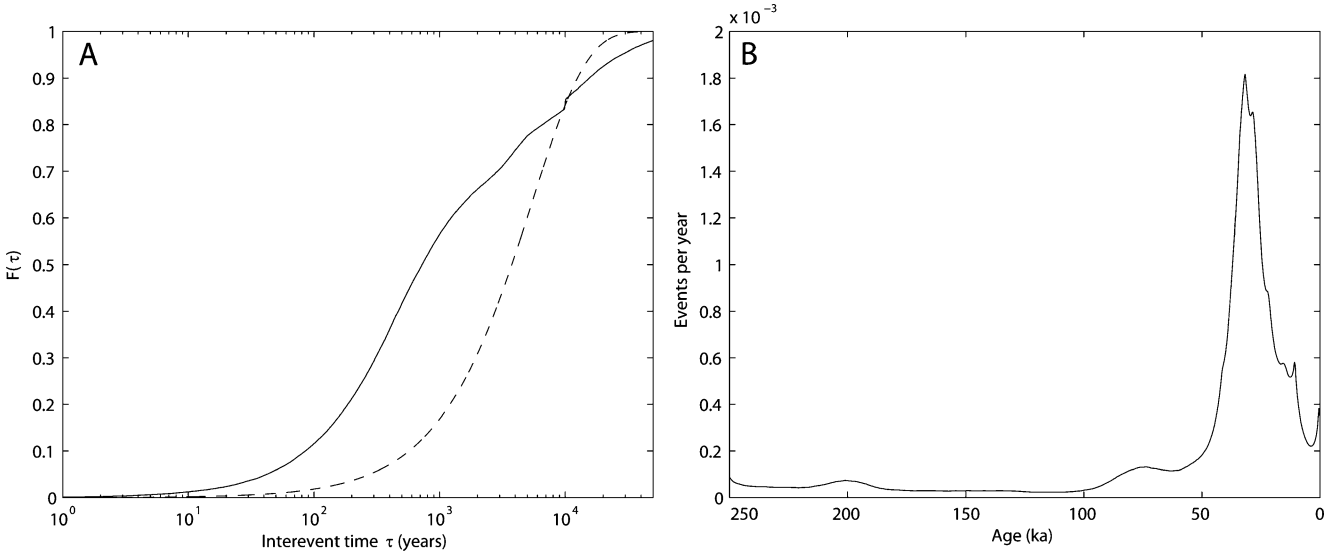

Fig. 9 **a** Distribution of times between successive events; and **b** a kernel-smoothed estimate of the time-varying eruption onset rate (Turner et al. 2008a). The *dashed line* in **a** is the reference line from an exponential distribution (a Poisson process)

Poisson process with a 'background rate' μ. Further, suppose that the occurrence of an eruption in the recent past raises the likelihood of a further eruption, with an effect that declines over time. The point process intensity (see, for example, Daley and Vere-Jones 2003) can then be written as

$$\lambda(t) = \mu + \nu \sum_{j:t_j<t} g(t - t_j), \tag{2}$$

where the probability (conditional on the history of the process) of an event in the time interval $(t,t+\Delta t)$ will be approximately $\lambda(t)\Delta t$, for small Δt. We require $\nu \int_0^\infty g(s)ds < 1$ to ensure that the process remains stable, i.e., that each event produces less than one additional event on average.

The point process intensity (Eq. 2) is the 'self-exciting' model of Hawkes (1971), subsequently applied to earthquakes by Hawkes and Adamopoulos (1973), Vere-Jones and Ozaki (1982), and Ogata (1988). For the excitation function g, physical considerations require that it be monotonically decreasing, and not have an artificial hard cut-off. Hence we will use

$$g(s) = \frac{1}{\sigma} \exp\left(-\frac{s^2}{2\sigma^2}\right),$$

the probability density function of a half-normal random variable with mean $\sigma\sqrt{2/\pi}$, which means that the stability condition becomes $\nu<1$. Thus the effect declines in a sigmoid fashion, in contrast to the exponential [$g(s) = \exp(-\eta s)$] and hyperbolic [$g(s) = s^{-p}$] decays used for earthquake aftershock sequences. This difference is driven by the structure of the data; with volcanic data at this resolution we are unable to separate eruptions close together in time, and volcanic eruptions do not occur in accordance with an Omori-type law, where the rate of triggered events declines as the reciprocal of the elapsed time. The parameters μ, ν and σ can be estimated using maximum likelihood, where the loglikelihood is

$$\log \mathrm{L} = \sum_{i=1}^{N} \log \lambda(t_i) - \int_{T_1}^{T_2} \lambda(t)dt.$$

An example for 1000 Monte Carlo realizations of the dating algorithm is shown in Fig. 10. The parameter estimates are μ=0.000059±0.000007/year, ν=0.71±0.04/year, and σ =3161±711 years. This means that the additional contribution to the rate from a previous event starts at 0.00022/year, and declines to 0.0001/year after 4021 years, and 0.00005/year after 5,479 years. Hence the contribution to the present day hazard from Rangitoto is still considerable (Fig. 10b).

While there are some visual differences between the intensities in Fig. 10a, it must be remembered that while the point intensity is calculated only from the past events, the kernel estimate 'looks ahead' to have a contribution from events that occur in the following few thousand years. Also, it is quite possible that some of the poorly constrained events in Table 3 actually occurred in batches, which is not reflected in the Monte Carlo simulation algorithm.

Spatial component of hazard

Spatial effects seem to be from the field as a whole; hence we considered a spatial density kernel (Connor and Connor 2009). The intensity at a point x is estimated as

$$f(x) = \frac{1}{2\pi\sqrt{|\mathrm{H}|}} \sum_{i=1}^{N} \exp\left(-\frac{1}{2}(x - x_i)^{\mathrm{T}}\mathrm{H}^{-1}(x - x_i)\right)$$

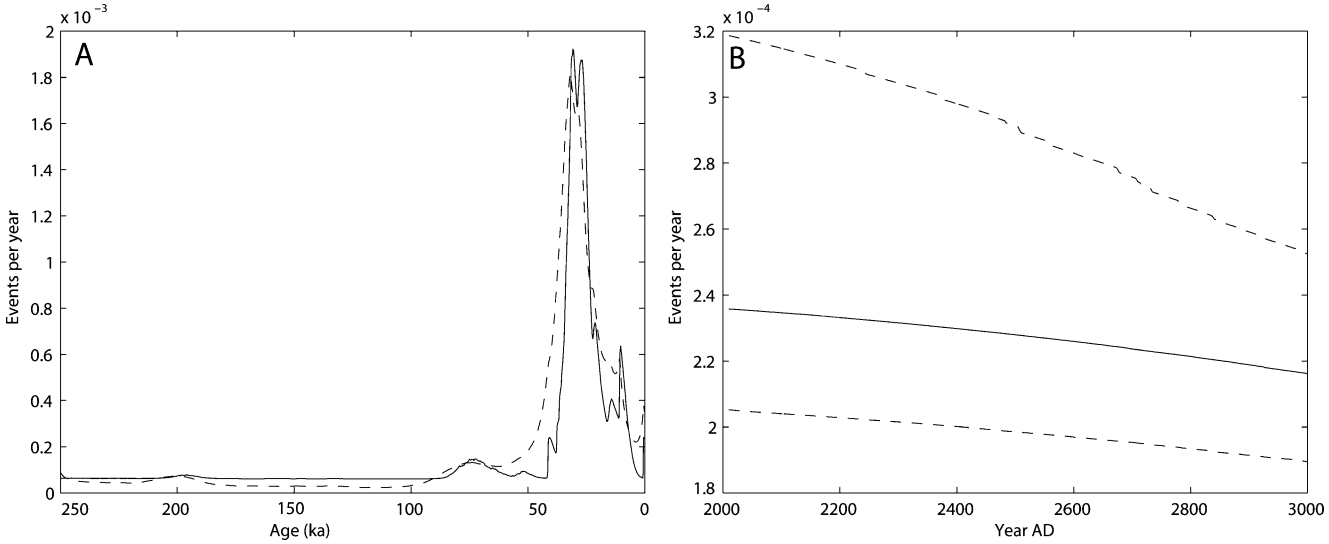

Fig. 10 **a** Kernel-smoothed estimate of the time-varying eruptive onset intensity (*dashed line*) and average fitted triggering intensity (*solid line*) for 1000 Monte Carlo realizations of the new age model. **b** Forecast intensity (*solid line*) and 90% confidence bound (*dashed lines*)

where the bandwidth matrix H is estimated using least squares cross validation (Duong 2007) as

$$\mathrm{H} = \begin{bmatrix} 10.0 & 16.8 \\ 16.8 & 30.0 \end{bmatrix}, \text{ and hence } \sqrt{\mathrm{H}} = \begin{bmatrix} 2.1 & 2.4 \\ 2.4 & 4.9 \end{bmatrix} \mathrm{km}.$$

This indicates east–west and north–south smoothing distances of 4.2 and 9.8 km, respectively, and a clockwise rotation of the kernel. In other words, there is a strong NE-SW spatial structure evident in the AVF (Fig. 11).

Discussion and conclusions

The development of the new age model presented here was made possible by the correlation of tephra layers with the

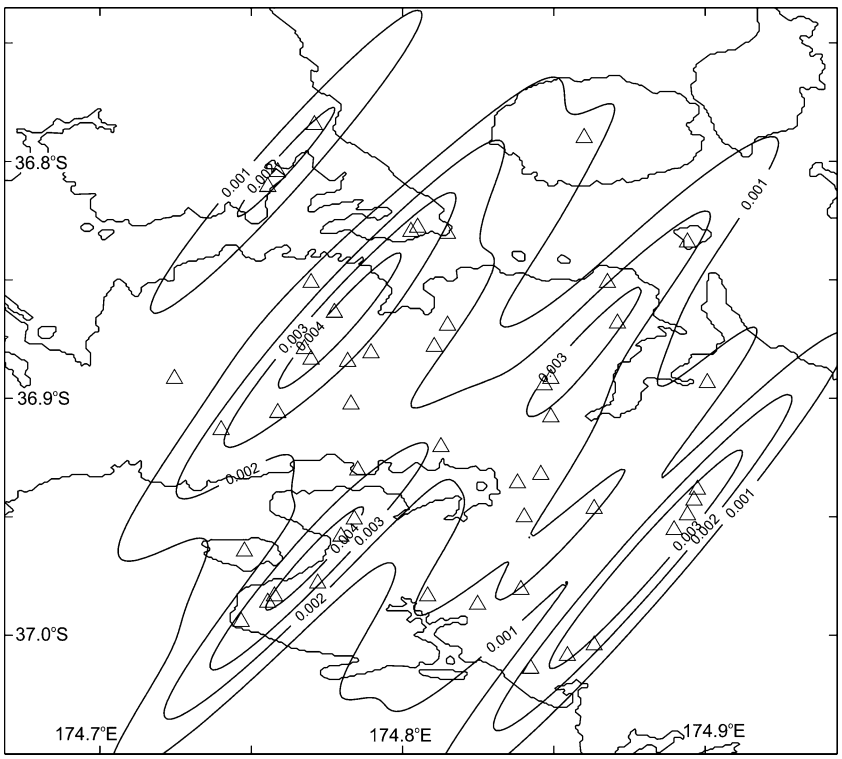

Fig. 11 Kernel-smoothed estimate of the spatial intensity of eruption sites in the AVF, probability contours at intervals of 0.001. *Triangles* represent eruption centres

AVF eruption centres based on their preserved thicknesses, the known pyroclastic volume of the eruption centres, and their location with respect to the core site. All of these are carried out within the known centre-age constraints. There is the potential for miscorrelations in our approach due to: 1) the potential of reworking and hence possible thickening or thinning of individual tephras in the cores (as commented on by Molloy et al. 2009), compared to an idealised fall thickness; 2) specific wind directions during eruption events producing narrowly distributed and elongate tephra fall thickness attenuations; and 3) that single eruption centres may have produced more than one tephra layer, as recognised for the most recent centres of the field, Mt Wellington and Rangitoto (Searle 1962; Horrocks et al. 2005a). Further work to test and develop this model hence requires a geochemical or petrological approach that extends beyond the problematic broad compositional ranges reported for glass chemistry from the field (e.g., Shane and Smith 2000). Examining component lithologies of tephra particles may also help add another layer of constraint, e.g., Molloy et al. (2009) recognise that AVF6-9 contain large proportions of accidental (non-volcanic) rock fragments, implying deposits from phreatomagmatic eruptions.

Under this new age model, the conclusion of Magill et al. (2005) that there is significant spatio-temporal clustering can be refuted. Instead the data suggest that spatial and temporal eruption recurrences in the AVF are independent of one another. Hence the location of the past event may not shed any light on the location of the next. The age data for events in the field are, however, only strong for the record since 50 ka ago, even with the additional core-tephra information. Older deposits' ages are still very poorly constrained by radiometric dating; further work is needed to provide information about the earlier development of the volcanic field.

Past workers have described the activity of the field as being 'spasmodic' (Cassidy et al. 1999) with episodes of high intensity separated by long pauses. Through geomagnetic work, the propensity for the field to produce rapid sequences of up to five disparate eruptions over periods of less than 100 years was confirmed (Cassata et al. 2008). Independently, the analysis of tephras within sediment cores from the field has also revealed periods of high eruption event intensity, including a major "flare-up" in explosive activity at 32±2 ka (Molloy et al. 2009). Our new age-order analysis clearly shows a strong numerical dominance of known events from the field in the period 40–20 ka (Fig. 10), confirming this 'flare-up' behaviour. This period accounts for over 63% of the known eruptions from the AVF, occuring within only 8% of the field's total life. Before this period, there is a period at least 160 ka long over which 10–12 eruptions are distributed, with the limited information available suggesting that many of them occurred concurrently at the inception of the field. The latest 20 ka includes up to 8 eruptions from only six eruptive centres, including the latest event that erupted a volume of magma equivalent to that produced collectively by all eruptions that had occurred before (Allen and Smith 1994). Based on this highly variable history, it can be assumed that there is no 'steady-state' approximation that can be applied to the eruption intensity or hazard at the AVF. Instead, its behaviour appears to have been controlled by a few times during which magma-supply rates were sharply higher, with the latest high-supply event being focused in a single eruption, and concentrated at a single point source.

Our results suggest that the spatial hazard intensity, or the spatial probability of vent opening, is strongly structurally controlled with a NE-SW orientation that is parallel to the strike of the subduction zone c. 500 km to the east, and to the orientation of the Taupo Volcanic Zone, dominating the Central North Island to the south (Fig. 1). This orientation is also sub-parallel to many North Island fault systems of the region to the south and east (Edbrooke 2001). The trend is perpendicular to regional magnetic and gravity anomalies of c. 340° to 325° representing the crustal structure (Spörli and Eastwood 1997), and may relate to their proposal that the AVF lies within a releasing structure of a dextral strike-slip regime.

In a global context, the AVF is a very small field with a relatively short geological history. In longer lived volcanic field systems, eruption intensity is also recognised to vary considerably over time, with pulses of high intensity much shorter than the million-year timescales of field life (e.g., Condit and Connor 1996). In these longer-lived systems, however, dating resolution does not allow the degree of analysis afforded at Auckland. Hence, the AVF data may represent a window onto a "pulsing" behaviour of major longer-lived volcanic fields, and shows that pulsatory magma supply on a range of temporal scales appears to characterise the behaviour of monogenetic volcanic fields.

Acknowledgements We wish to acknowledge support by the NZ FRST-IIOF Grant "Facing the challenge of Auckland's Volcanism" (MAUX0808). We thank Jan Lindsay and Ian Smith (U of Auckland) for valuable discussion on event ages and other features of the AVF and Kate Arentsen (Massey U) for comments on the manuscript. Reviews by Olivier Jaquet and an anonymous referee led to important improvements in the paper.

References

Adams M (1986) Thermoluminescence dating of plagioclase feldspar. Unpubl MSc Thesis, U Auckland. 104p

Affleck DK, Cassidy J, Locke CA (2001) Te Pouhawaiki Volcano and pre-volcanic topography in central Auckland: volcanological and hydrological implications. NZ J Geol Geophys 44:313–321

Allen SR, Smith IEM (1994) Eruption styles and volcanic hazard in the Auckland Volcanic Field, New Zealand. Geosci Rep Shizuoka Univ 20:5–14

Bebbington M (2007) Identifying volcanic regimes using hidden Markov models. Geophys J Int 171:921–942

Bebbington M (2008) Incorporating the eruptive history in a stochastic model for volcanic eruptions. J Volcanol Geotherm Res 175:325–333

Bebbington M (2010) Trends and clustering in the onsets of volcanic eruptions. J Geophys Res 115:B01203. doi:10.1029/2009JB006581

Bebbington MS, Lai CD (1996) On nonhomogeneous models for volcanic eruptions. Math Geol 28:585–600

Cassata WS, Singer BS, Cassidy J (2008) Laschamp and Mono Lake geomagnetic excursions recorded in New Zealand. Earth Planet Sci Lett 268:76–88

Cassidy J (2006) Geomagnetic excursion captured by multiple volcanoes in a monogenetic field. Geophys Res Lett 33:L21310

Cassidy J, Locke CA, Miller CA, Rout DJ (1999) The Auckland volcanic field, New Zealand: geophysical evidence for its eruption history. In: Firth CG, McGuire WJ (eds) Volcanoes in the Quaternary. Geol Soc Lond Spec Publ 161: 1–10

Condit CD, Connor CB (1996) Recurrence rates of volcanism in basaltic volcanic fields: an example from the Springerville volcanic field, Arizona. Geol Soc Am Bull 108:1225–1241

Connor CB, Connor LJ (2009) Estimating spatial density with kernel methods. In: Connor CB, Chapman NA, Connor LJ (eds) Volcanic and tectonic hazard assessment for nuclear facilities. Cambridge University Press, Cambridge, UK, pp 346–368

Connor CB, Conway FM (2000) Basaltic volcanic fields. In: Sigurdsson H, Houghton BF, McNutt SR, Rymer H, Stix J, Ballard RD (eds) Encyclopedia of volcanoes. Academic, San Diego, pp 331–343

Connor CB, Hill BE (1995) Three nonhomogeneous Poisson models for the probability of basaltic volcanism: application to the Yucca Mountain region, Nevada. J Geophys Res 100:10107–10125

Connor CB, Stamatakos JA, Ferrill DA, Hill BE, Ofoegbu GI, Conway FM, Sagar B, Trapp J (2000) Geological factors controlling patterns of small-volume basaltic volcanism: application to a volcanic hazards assessment at Yucca Mountain, Nevada. J Geophys Res 105:417–432

Conway FM, Connor CB, Hill BE, Condit CD, Mullaney K, Hall CM (1998) Recurrence rates of basaltic volcanism in SP cluster, San Francisco volcanic field, Arizona. Geology 26:655–658

Cronin S, Bebbington M, Lai CD (2001) A probabilistic assessment of eruption recurrence on Taveuni volcano, Fiji. Bull Volcanol 63:274–288

Daley DJ, Vere-Jones D (2003) An introduction to the theory of point processes. Volume 1, 2nd edn. Springer, New York, 469 p

Duong T (2007) ks: kernel density estimations and kernel discriminant analysis for multivariate data in R. J Statist Softw 21(7):1–16

Eade J (2009) Petrology and correlation of lava flows from the central part of the Auckland Volcanic Field. Unpubl MSc thesis, U Auckland

East GRW, George AK (2003) The construction of the Auckland Central Remand Prison on the Mt Eden basalt flow. In: Crawford SA, Baunton P, Hargraves S (eds) Geotechnics on the volcanic edge. Institution of Professional Engineers NZ, Wellington, pp 387–396

Edbrooke SW (2001) Geology of the Auckland area. Institute of Geological and Nuclear Sciences 1:250 000 Geological Map 3. 1 sheet + 74p. GNS Science, Lower Hutt

Fergusson G, Rafter TA (1959) New Zealand C14 age measurements—4. NZ J Geol Geophys 2:208–241

Firth CW (1930) The geology of the north-west portion of Manukau County, Auckland. Trans Roy Soc NZ 61:85–137

Grant-Taylor TC, Rafter TA (1963) New Zealand natural radiocarbon measurements I–V. Radiocarbon 5:118–162

Grant-Taylor TC, Rafter TA (1971) New Zealand radiocarbon age measurements—6. NZ J Geol Geophys 14:364–402

Grenfell H, Kenny JA (1995) Another piece in the Auckland Volcanic Field jigsaw puzzle—or are we stumped? Geol Soc NZ Newsl 107:42–43

Hasenaka T, Carmichael ISE (1985) The cinder cones of Michoacàn-Guanajuato, central Mexico: their age, volume and distribution, and magma discharge rate. J Volcanol Geotherm Res 25:105–124

Hayward BW (2008) Ash Hill Volcano, Wiri. Geocene 3:8

Hawkes AG (1971) Spectra of some self-exciting and mutually exciting point processes. Biometrika 58:83–90

Hawkes A, Adamopoulos L (1973) Cluster models for earthquakes—regional comparisons. Bull Int Stat Inst 45:454–461

Hill BE, Connor CB, Jarzemba MS, La Femina PC, Navarro M, Strauch W (1998) 1995 eruptions of Cerro Negro volcano, Nicaragua, and risk assessment for future eruptions. Geol Soc Amer Bull 110:1231–1241

Horrocks M, Augustinus P, Deng Y, Shane P, Andersson S (2005a) Holocene vegetation, environment, and tephra recorded from Lake Pupuke, Auckland, New Zealand. NZ J Geol Geophys 48:85–94

Horrocks M, Nichol SL, D'Costa DM, Shane P, Prior C (2005b) Paleoenvironment and human impact in modifying vegetation at Mt St John, Auckland isthmus, New Zealand. NZ J Bot 43:211–221

Kermode LO (1992) Geology of the Auckland urban area. Scale 1:50 000. Institute of Geological and Nuclear Sciences geological map 2. 1 sheet + 63p. GNS Science, Lower Hutt

Kermode LO, Smith IEM, Moore CL, Stewart RB, Ashcroft J, Nowell SB, Hayward BW (1992) Inventory of Quaternary volcanoes and volcanic features of Northland, South Auckland and Taranaki. Geol Soc NZ Misc Publ 61. 100 p

Kienle J, Kyle PR, Self S, Motyka RJ, Lorenz V (1980) Ukinrek Maars, Alaska: I. April 1977 eruption sequence, petrology and tectonic setting. J Volcanol Geotherm Res 7:11–37

Lindsay J, Leonard G (2009) Age of the Auckland Volcanic Field. Inst Earth Sciences and Engineering Report 1-2009.02, U Auckland, NZ, 38p

Lowe DJ, Shane PAR, Alloway BR, Newnham RW (2008) Fingerprints and age models for widespread New Zealand tephra marker beds erupted since 30,000 years ago: a framework for NZ-INTIMATE. Quatern Sci Rev 27:95–126

Magill C, Blong R (2005) Volcanic risk ranking for Auckland, New Zealand. I: methodology and hazard investigation. Bull Volcanol 67:331–339

Magill CR, McAneney KJ, Smith IEM (2005) Probabilistic assessment of vent locations for the next Auckland volcanic field event. Math Geol 37:227–242

Magill CR, Hurst AW, Hunter LJ, Blong RJ (2006) Probabilistic tephra fall simulation for the Auckland Region, New Zealand. J Volcanol Geotherm Res 153:370–386

Martin AJ, Umeda K, Connor CB, Weller JN, Zhao D, Takahashi M (2004) Modeling long-term volcanic hazards through Bayesian inference: an example from the Tohoku volcanic arc, Japan. J Geophys Res 109:B10208

McDougall I, Polach HA, Stipp JJ (1969) Excess radiogenic argon in young sub-aerial basalts from the Auckland volcanic field, New Zealand. Geochim Cosmochim Acta 33:1485–1520

Mochizuki N, Tsunakawa H, Shibuya H, Tagami T, Ozawa A, Cassidy J, Smith IEM (2004) K–Ar ages of the Auckland geomagnetic excursions. Earth Planet Space 56:283–288

Molloy C, Shane P, Augustinus P (2009) Eruption recurrence rates in a basaltic volcanic field based on tephra layers in maar sediments: implications for hazards in the Auckland volcanic field. GSA Bull 121:1666–1677

Newnham RM, Lowe DJ, Alloway BV (1999) Volcanic hazards in Auckland, New Zealand: a preliminary assessment of the threat

posed by central North Island silicic volcanism based on the Quaternary tephrostratigraphical record. In: Volcanoes in the Quaternary, Firth C, McGuire WJ (eds). Special Publ 161, Geol Soc London; 27–45

Newnham RM, Lowe DJ, Giles T, Alloway BV (2007) Vegetation and climate of Auckland, New Zealand, since ca. 32 000 cal. yr ago: support for an extended LGM. J Quatern Sci 22:517–534

Ogata Y (1988) Statistical models for earthquake occurrences and residual analysis for point processes. J Am Stat Assoc 83:9–27

Phillips S (1989) Aspects of thermoluminescence dating of plagioclase feldspar. Unpubl MSc thesis, U Auckland. 39p

Polach HA, Chappell J, Lovering JF (1969) Australian National University radiocarbon date list. Radiocarbon 11:245–262

Reid SJ (1980) Frequencies of low-level free atmospheric wind flows in northern and southern New Zealand. New Zealand Meteorological Service, Wellington

Rhoades DA, Dowrick DJ, Wilson CJN (2002) Volcanic hazard in New Zealand: scaling and attenuation relations for tephra fall deposits from Taupo Volcano. Nat Hazards 26:147–174

Rout DJ, Cassidy J, Locke CA, Smith IEM (1993) Geophysical evidence for temporal and structural relationships within the monogenetic basalt volcanoes of the Auckland volcanic field, northern New Zealand. J Volcanol Geotherm Res 57:71–83

Sameshima T (1990) Chemical and dating data on some of the monogenetic volcanoes of Auckland. Geol Soc NZ Annual Conference Nov 1990, Napier, Programme and Abstracts. p118

Sandiford A, Alloway B, Shane P (2001) A 28 000–6600 cal yr record of local and distal volcanism preserved in a paleolake, Auckland, New Zealand. NZ J Geol Geophys 44:323–336

Sandiford A, Horrocks M, Newnham R, Ogden J, Alloway B (2002) Environmental change during the last glacial maximum (c. 25 000–c. 16 500 years BP) at Mt Richmond, Auckland Isthmus, New Zealand. J R Soc NZ 32:155–167

Searle EJ (1959a) Pleistocene and Recent studies of Waitemata Harbour: Part 2—North Shore and Shoal Bay. NZ J Geol Geophys 2:95–107

Searle EJ (1959b) The volcanoes of Ihumatao and Mangere, Auckland. NZ J Geol Geophys 2:870–888

Searle EJ (1961) The age of the Auckland volcanoes. NZ Geogr 17:52–63

Searle EJ (1962) The volcanoes of Auckland City. NZ J Geol Geophys 5:193–227

Searle EJ (1964) City of volcanoes. A geology of Auckland. Longman Paul, Auckland, 112p

Searle EJ (1965) Auckland volcanic district. NZ Dept Sci Ind Res Info Ser 49:90–103

Self S, Kienle J, Huot J-P (1980) Ukinrek Maars, Alaska: II. Deposits and formation of the 1977 craters. J Volcanol Geotherm Res 7:39–65

Shane P (2005) Towards a comprehensive distal andesitic tephrostratigraphic framework for New Zealand based on eruptions from Egmont Volcano. J Quat Sci 20:45–57

Shane P, Hoverd J (2002) Distal record of multi-sourced tephra in Onepoto Basin, Auckland, New Zealand: implications for volcanic chronology, frequency and hazards. Bull Volcanol 64:441–454

Shane P, Sandiford A (2003) Paleovegetation of marine isotope stages 4 and 3 in northern New Zealand and the age of the widespread Rotoehu Tephra. Quat Res 59:420–429

Shane P, Smith IEM (2000) Geochemical characterisation of basaltic tephra deposits in the Auckland Volcanic Field. NZ J Geol Geophys 43:569–577

Sibson RH (1968) Late Pleistocene volcanism in the East Tamaki district. Unpubl BSc(Hons) thesis, U Auckland

Smith IEM, Blake S, Wilson CJN, Houghton BF (2008) Deep-seated fractionation during the rise of a small-volume basalt magma batch: Crater Hill, Auckland, New Zealand. Contrib Mineral Petrol 155:511–527

Smith IEM, McGee LE, Lindsay JM (2009) Review of the petrology of the Auckland Volcanic Field. Institute of Earth Science and Engineering Report, 1-2009.03. IESE, Auckland, 36p

Spörli KB, Eastwood VR (1997) Elliptical boundary of an intraplate volcanic field, Auckland, New Zealand. J Volcanol Geotherm Res 79:169–179

Takada A (1994) The influence of regional stress and magmatic input on styles of monogenetic and polygenetic volcanism. J Geophys Res 99:13563–13574

Turner M, Cronin S, Smith I, Bebbington M, Stewart RB (2008a) Using titanomagnetite textures to elucidate volcanic eruption histories. Geology 36:31–34

Turner M, Cronin S, Bebbington M, Platz T (2008b) Developing a probabilistic eruption forecast for dormant volcanos; a case study from Mt Taranaki, New Zealand. Bull Volcanol 70:507–515

Turner M, Bebbington M, Cronin S, Stewart RB (2009) Merging eruption datasets: building an integrated Holocene eruptive record of Mt Taranaki. Bull Volcanol 71:903–918

Valentine GA, Gregg TKP (2008) Continental basaltic volcanoes—processes and problems. J Volcanol Geotherm Res 177:857–873

Vere-Jones D, Ozaki T (1982) Some examples of statistical inference applied to earthquake data. Ann Inst Stat Math 34:189–207

Von Veh MW, Nemeth K (2009) An assessment of the alignments of vents on geostatistical analysis in the Auckland Volcanic Field, New Zealand. Géomorphol Relief Processus Environment 3:175–186

Ward GK, Wilson SR (1978) Procedures for comparing and combining radiocarbon age determinations: a critique. Archaeometry 20: 19–31

Wood IA (1991) Thermoluminescence dating of the Auckland and Kerikeri basalt fields. Unpubl MSc thesis, U Auckland. 141p